Enhanced Sintering of an Fe-Ni-P Coated Composite Powder Prepared by Electroless Nickel Plating

T.-Y. Chan and S.-T. Lin

An Fe-8.2%Ni-6.0%P powder was prepared by electroless nickel plating on a carbonyl iron powder, where phosphorous appeared as a contaminant of the plating process. Because of the high phosphorous concentration, persistent liquid phase sintering was effective at temperatures higher than 1000 °C. The sintered microstructure was dramatically different from the conventional approaches, where a low concentration of phosphorous was added in the form of Fe_3P. Sintering the alloy at a temperature as low as 1050 °C for 30 min yielded a sintered density of 98.6% theoretical and rounded grains having an average grain size of 53 μm. The rounded grains were surrounded by a large volume fraction of intergranular $(Fe,Ni)_3P$ phase, arising from the high phosphorous concentration, which slightly deteriorated the magnetic saturation but significantly increased the electrical resistivity of the alloy. Generally speaking, the magnetic saturation of the sintered alloy was improved with respect to the iron-phosphorus, iron-nickel, or iron-silicon alloys fabricated by powder processing.

Keywords coated composite powder, Fe-Ni-P ternary alloy, liquid phase sintering, magnetic properties

1. Introduction

Powder metallurgy process lends itself well for economical mass production of complicated soft magnetic components. The drawbacks of the sintered materials are, however, relatively poor and erratic magnetic characteristics due to the existence of a large amount of residual porosity. Different soft magnetic alloys, including iron-silicon, iron-nickel, and iron-phosphorus, having intricate geometries are manufactured by this process route (Ref 1-6). Among these soft magnetic materials, fully dense iron-nickel alloys have relatively high initial and maximum permeabilities (Ref 7). However, sintering of iron-nickel powder mixtures is impeded by the closely packed face-centered cubic structure because nickel is an austenite stabilizer. For example, sintering fine iron-nickel powder mixtures at a temperature as high as 1350 °C for 1 h only yielded about 90% theoretical density and yet with inhomogeneous distribution of iron and nickel, resulting in deteriorated magnetic properties (Ref 8).

As there is no liquid phase to aid the atomic transport in the iron-nickel system at a temperature as high as 1350 °C, the temperature-enhanced solid-state diffusion of these two substitutional elements is the primary mechanism for material transfer. The alternative approach to solve this problem is to incorporate a metalloid element into the system to enhance material transfer, but without deterioration of the properties of the sintered alloys. Phosphorous has been added to various iron-base material systems to enhance the sintering rate of iron powder compacts because it is a ferrite stabilizer and forms a eutectic phase with iron at 1048 °C (Ref 1-5). Increase of grain size, coagulation of impurities to the grain boundaries, and rounding of pores are the consequences of phosphorous alloying, which in turn results in favorable influences on the magnetic properties of the sintered alloys. In addition, homogenization of alloying elements can be achieved at lower temperatures, such as in the case of iron-silicon alloys where the homogenization temperature of elements can be achieved at a temperature as low as 1100 °C for 1 h (Ref 9). Therefore, it can be expected that the obstacles associated with sintering elemental iron-nickel powder mixtures can possibly be minimized with the addition of phosphorous.

The distribution homogeneity of the minor components in the powder state determines the sintering behavior and, therefore, the properties and consistency of the sintered products (Ref 10, 11). Present techniques in powder metallurgy industries for the manufacturing of composite powders use prealloyed or mixed individual powders. As an alternative, the coating of metal powder particles with a uniform adhesive layer of the alloying elements by electroless plating has generated considerable interest recently (Ref 12, 13). This technique avoids the problems associated with the mixed individual powders by reducing diffusion distances during sintering. Densification is more isotropic, which is vital to the production of net-shape components by powder processing techniques (Ref 10).

The goal of this study was to adopt an electroless nickel plating technique to prepare coated composite powders using a phosphorous-base bath composition. Electroless nickel plating is a very common technique for preparing protective coatings on workpieces in the metal-finishing industry. Various formulations exist for electroless nickel plating, which are composed of different nickel salts, reducing agents, and stabilizers. The general mechanism for the reaction is as follows (Ref 12, 14):

$$Ni^{2+} + [\text{Reducing agent}] + [\text{Stabilizer}] + [\text{pH buffer}] \rightarrow$$
$$Ni + H_2 + [\text{Contaminant}] + [\text{Soluble products}]$$

The species and concentrations of the reducing agent and stabilizer, pH value, and temperature of the bath solution control the deposition rate and content of phosphorous contamination.

T.-Y. Chan, Mechanical Engineering Department, Far-East College, Tainan, Taiwan; and **S.-T. Lin,** Mechanical Engineering Department, National Taiwan University of Science and Technology, Taipei, Taiwan, e-mail: stlin@mail.ntust.edu.tw.

2. Experimental Procedures

A nickel salt in solution was autocatalytically reduced to coat suspended carbonyl iron powder. The base powder was a carbonyl iron powder (OM grade, BASF, Germany), which had a mean particle size of 4 μm. The major impurities of this powder were carbon (0.74%), nitrogen (0.66%), and oxygen (0.15%). To improve the results of electroless plating, the as-received powder was treated with an acidic water solution prior to plating. Initially, the powder was immersed in a 1% diluted HCl aqueous solution, maintained at 50 °C, for 10 min. The weight ratio of powder to the aqueous solution was 7 to 20. The powder was then washed with distilled water and subsequently acetone. Finally, the powder was dried in vacuum oven at 60 °C for 2 h.

Electroless plating was carried out using an acidic type solution maintained at 90 °C. This bath solution was prepared by dissolving 20 g of nickel sulfate ($NiSO_4 \cdot 6H_2O$), 27 g of sodium hypophosphite ($NaH_2PO_2 \cdot H_2O$), and 16 g of sodium succinate ($Na_2C_4H_4O_4 \cdot 6H_2O$) in 1000 cm^3 diluted H_2SO_4 aqueous solution. The initial pH value of the solution was 5. The powder was poured into the bath solution and stirred for 30 min. The plated powder was then washed and dried according to the same procedures executed prior to plating.

The composite powder was wet milled, together with 2 wt% paraffin wax, in heptane for 12 h. The milled powder was then dried, granulated, and sieved with 170 mesh screen. Green specimens having the dimensions of 12 mm in diameter and 13 mm in height were uniaxially pressed under a pressure of 100 MPa. The specimens were then sintered in dry hydrogen (dew point = −50 °C) at either 1000, 1050, or 1100 °C for 30 min. The sintered density was measured using the water-immersion method, while hardness was tested using a Rockwell hardness tester on the A scale. Phase analysis of the bulk sintered specimens was performed using x-ray diffraction (XRD) (Rigaku DMAX-B; Tokyo, Japan) with Cu(Kα) radiation at an accelerating voltage of 40 keV. Morphological analysis of the sintered microstructure was carried out using both optical microscope and scanning electron microscope (SEM) (Cambridge, S360; Cambridge, UK) at an accelerating voltage of 20 keV. Magnetic properties were measured using magnetic hysteresis loop tracer (YOKOGAWA 3257; Tokyo, Japan).

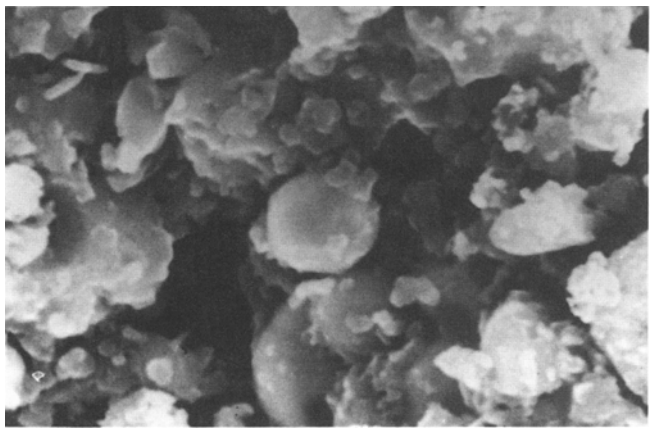

Fig. 1 Scanning electron micrograph of the electroless nickel plated carbonyl iron powder in the as-coated state

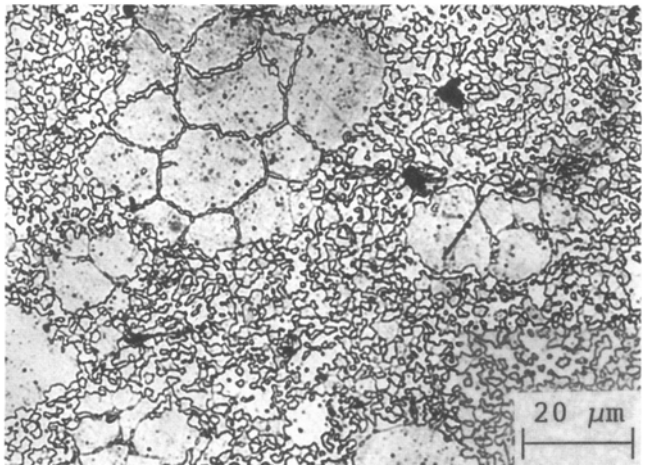

(a)

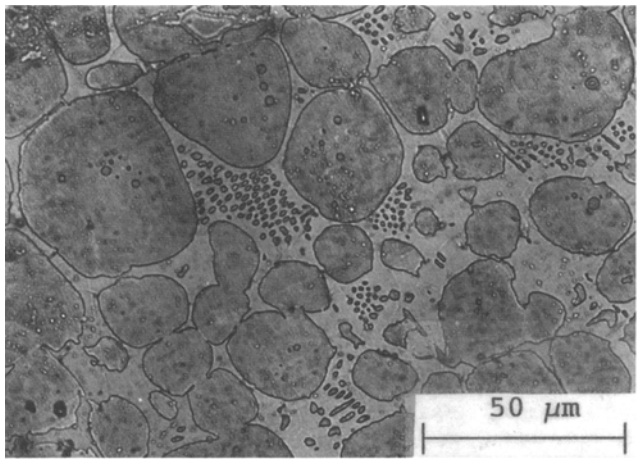

(b)

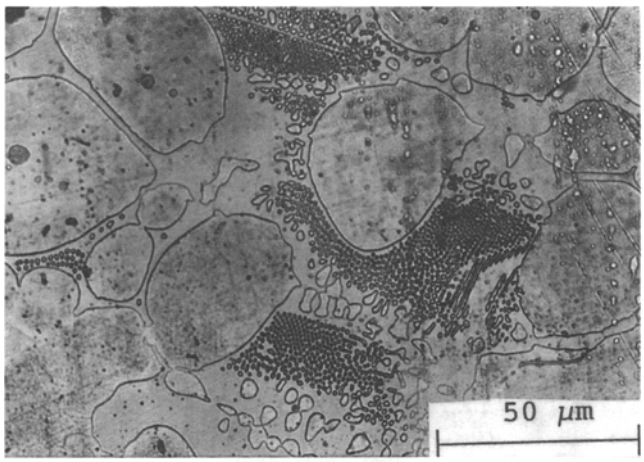

(c)

Fig. 2 Evolution of microstructure with increase of sintering temperature. (a) 1000 °C. (b) 1050 °C. (c) 1100 °C

3. Results and Discussion

Figure 1 shows an SEM micrograph of the composite powder in the as-coated state. The plating procedures used in this study did not result in an evenly coated layer. Instead, the crystals of the coated materials were finely distributed among the carbonyl iron particles. The overall composition of this composite powder was Fe-8.2%Ni-6.0%P by weight, determined by inductively coupled plasma mass spectrometry. The phosphorous concentration was unexpectedly higher than the maximum solubilities of phosphorous in iron and nickel, which are 2.8 and 0.17 wt% at the binary eutectic temperatures of 1048 and 870 °C, respectively (Ref 15). For Fe-Ni-P ternary alloys at 970 °C, the maximum solubilities of phosphorous in Fe-4.1%Ni and Fe-12.5%Ni are 2.0 and 2.8 wt%, respectively (Ref 16). Thus, with linear interpolation, the maximum solubility of phosphorous in Fe-8.2%Ni is about 2.4 wt% at 970 °C. In comparison, it was generally believed that the optimal concentration of phosphorous lay between 0.8 and 1.2 wt% for iron-phosphorus alloys prepared by powder sintering (Ref 1, 2). With a phosphorous concentration of 1.8 wt% or above, essentially all grain boundaries showed secretions of Fe_3P (Ref 3, 4). As the phosphorous concentration of the composite powder prepared in this study was much higher than its solubility in the matrix phase, it was expected that different forms of iron-nickel phosphides would precipitate after sintering, resulting in deterioration of magnetic properties of the sintered alloy.

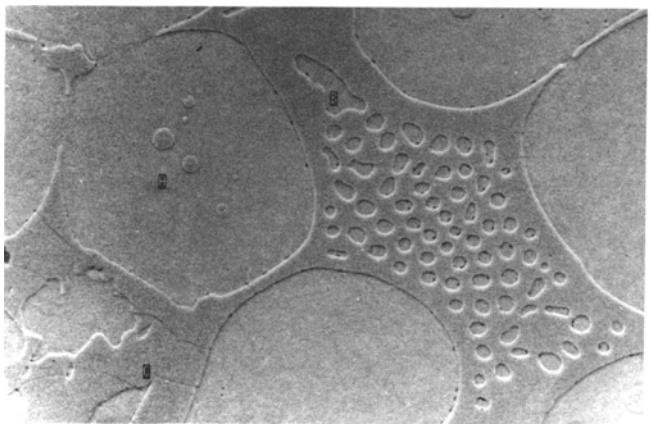

Fig. 3 Etched micrograph for a sample sintered at 1050 °C

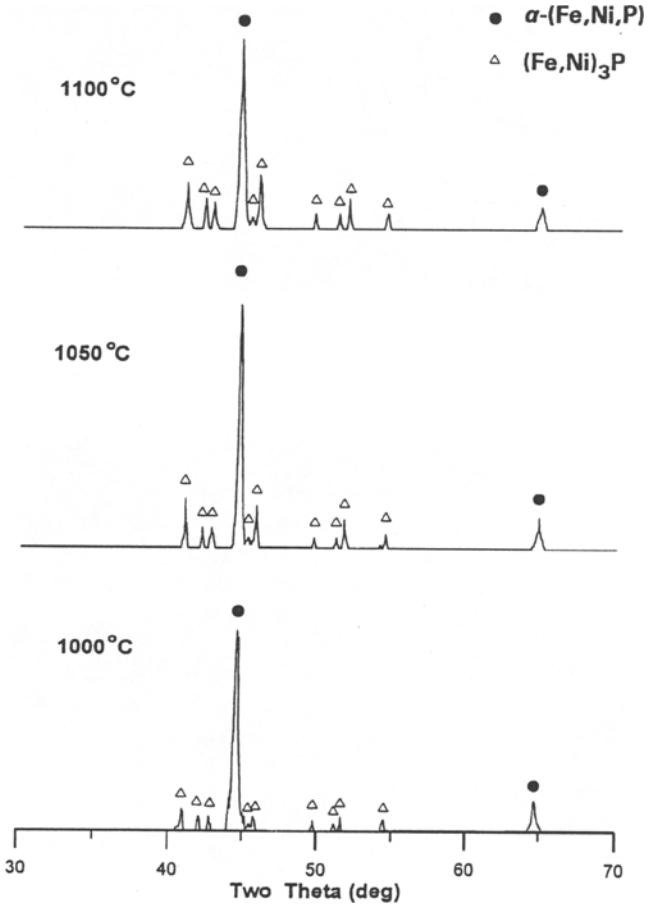

Fig. 4 X-ray diffraction patterns for Fe-8.2%Ni-6.0%P sintered at different temperatures, showing the existence of α(Fe,Ni,P) and $(Fe,Ni)_3P$ phases

Figure 2 shows the evolution of microstructure for the alloy sintered at various temperatures. There existed an intergranular phase that was in the liquid state during sintering. Thus, the sintering mechanism was persistent liquid phase sintering, in contrast to the transient liquid phase sintering for lower phosphorous concentration employed in conventional powder metallurgy methods. Because the sintering temperature of 1000 °C was lower than the eutectic temperature of iron-phosphorus (1048 °C), but higher than that of nickel-phosphorus (870 °C) (Ref 15), the relative abundance of the intergranular phase was much lower than alloys sintered at higher temperatures. In addition, triggering of exaggerated grain growth can be observed for the specimen sintered at 1000 °C, indicating that the coated layer was not evenly distributed on the carbonyl iron particle surface. With the formation of excessive liquid phase at higher temperatures, the grains tended to be rounded and residual pores can hardly be observed. However, at a sintering temperature of 1100 °C, the sample slumped due to the existence of a large volume fraction of liquid phase.

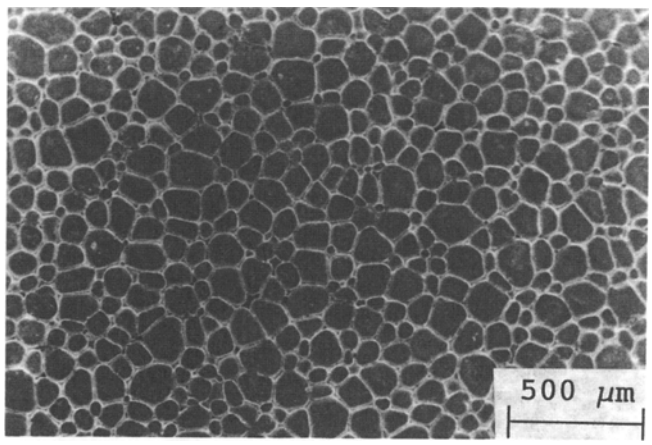

Fig. 5 Sintered microstructure for an electroless nickel plated carbonyl iron powder having a composition of Fe-21.3%Ni-2.7%P sintered at 1200 °C for 1 h, showing a close to fully dense microstructure yet with the lack of a large fraction of intergranular $(Fe,Ni)_3P$ phase

Figure 3 shows the SEM micrograph for an etched sample sintered at 1050 °C. There existed small precipitates within the grains and within the intergranular phase, which caused two different etched depths. Composition analysis based on energy-dispersive x-ray analysis (EDXA) indicated that the submerged area was composed of Fe-10.0%Ni-1.9%P, while the protruding area was composed of Fe-10.8%Ni-18.0%P. The phosphorous concentration in the submerged area was close to its saturated solubility in Fe-10%Ni, while that in the protruding area was close to the weight percentage of phosphorous in Fe_3P.

Figure 4 shows the XRD patterns for the alloys sintered at various temperatures. Only two discrete phases having lattice parameters close to those of αFe and Fe_3P were identified. According to previous analyses, these two phases were denoted as α(Fe,Ni,P) and $(Fe,Ni)_3P$, respectively.

Table 1 shows the variation of sintered properties with sintering temperature. Notable are the high magnetic saturation associated with the high sintered density and large grain size and the high hardness associated with the effects of solution hardening and precipitation hardening. In comparison, sintering Fe-2%Ni and Fe-3%Si at a temperature as high as 1316 °C yielded the magnetic saturations of 1.51 and 1.50 T, respectively (Ref 5, 6). Generally, the magnetic saturation of the sintered Fe-8.2%Ni-6.0%P alloy was much higher than those commonly quoted for the iron-nickel, iron-silicon, and iron-phosphorus alloys prepared by conventional powder metallurgy or metal injection molding (Ref 7). Nevertheless, the magnetic saturation achieved in this study was still lower than 2.15 T for theoretically dense pure iron (Ref 17).

For applications involving high-frequency operation, an increase in electrical resistivity reduces the eddy-current loss. In such applications, bulk iron-silicon alloys or laminated iron-silicon alloys are used extensively (Ref 7, 17). This trend is due to the fact that, with the alloying of 3 wt% Si, the electrical resistivity of iron increases substantially from 10 to 46 μΩcm, only at the sacrifice of decreasing its magnetic saturation from 2.15 to 2.02 T (Ref 17). In this study, because of the existence of an intergranular $(Fe,Ni)_3P$ phase, the electrical resistivity of the Fe-8.2%Ni-6.0%P alloy was much higher than those of different iron-silicon alloys (Ref 6, 7, 17). Consequently, Fe-Ni-P alloys pose the potential in high-frequency applications.

The micrographs shown in Fig. 2 indicate that a large volume fraction of intergranular $(Fe,Ni)_3P$ phase existed. With calculation based on the assumptions that the intergranular $(Fe,Ni)_3P$ phase had a density close to that of Fe_3P (6.74 g/cm^3) (Ref 18) and the maximum solubility of phosphorous in the solid solution of iron and nickel was 2.4 wt%, the volume fraction of the intergranular phase was 0.22. Such a large volume fraction of intergranular phase could have caused detrimental effects on the magnetic properties of this sintered composite. Fortunately, Fe_3P is a ferromagnetic material having a magnetic saturation of 1.29 T and a Curie temperature of 443 °C, but its magnetic properties are deteriorated with dissolution of Ni_3P (Ref 17). Therefore, the effects of the intergranular phase on the magnetic properties of the sintered alloy were not as detrimental as residual porosity. Estimation based on summing the fractional volumetric contribution from each phase yielded an ideal maximum magnetic saturation of 1.92 T for the fully densified Fe-8.2%Ni-6.0%P. Thus, with the existence of small precipitates within the grains and intergranular phase, the magnetic saturation of Fe-8.2%Ni-6.0%P sintered at 1050 °C was very close to this ideal value.

The soft magnetic properties of powder metal components are essentially dictated by the level of impurities within the grains or in the grain boundaries, sintered density, pore shape, and grain size. To achieve these optimal goals, increasing sintering temperature and sintering time, in addition to using an appropriate sintering atmosphere, were the general practices (Ref 1-5). Furthermore, it was shown that, for various methods of adding phosphorus to iron, the greatest magnetic properties were obtained when Fe_3P is used as the admixture (Ref 1, 3, 4). However, there still existed porosity within the grain or near the grain boundaries even at high sintering temperatures. For example, sintering Fe-0.8%P at 1277 °C for 24 h resulted in about 3% residual porosity within the grains, only yielding a magnetic saturation of 1.83 T (Ref 3).

The unexpectedly high phosphorous concentration in the coated composite powder was caused by the extreme sensitivity of phosphorous contamination to the pH value of bath solution. For example, using the same electroless plating parameters except the pH value of the bath solution, phosphorous contamination in the plated nickel layer decreased from 18 to 8 wt% as the pH value of the plating solution increased from 2 to 5 (Ref 14). Thus, to avoid the excessive coating of phosphorous on the iron powder, a bath solution with a higher pH value has to be used. One tentative test was carried out to study the feasibility of reducing the phosphorous concentration. In this test, the processing parameters were maintained the same as those carried out previously except that the pH value of the bath solution prior to plating was maintained at 6, instead of 5. This alternative test yielded a composite powder having a composition of Fe-21.3%Ni-2.7%P. The phosphorous concentration had been reduced to the content close to its solubility limit in iron-nickel alloys, but the concentration of nickel was surprisingly much higher than the first attempt. Figure 5 shows the microstructure of this alloy sintered at 1200 °C for 1 h. Clearly, a close to fully dense microstructure with large grains and

Table 1 Variation of sintered properties with sintering temperature

Sintering temperature, °C	Density (theoretical), %	Hardness, HRA	Magnetic saturation, T	Remenent inductance, T	Electrical resistivity, μΩcm	Average grain size, μm
1000	94.2	59	1.5	1.2	156	10
1050	98.6	69	1.7	1.4	161	53
1100	99.4	67	(a)	(a)	163	73

(a) Properties were not determined because the specimens slumped during sintering.

scarce intergranular phase was obtained. The magnetic properties are expected to be improved. Based on previous observations, it can be suggested that close control over the processing parameters has to be carried out to have consistent sintered results.

4. Conclusions

A coated composite iron powder having a high phosphorous concentration, arising from contamination during electroless nickel plating, proved effective in eliminating porosity and increasing grain size, yet also resulted in excessive abundance of intergranular $(Fe,Ni)_3P$ precipitation. The intergranular $(Fe,Ni)_3P$ phase slightly deteriorated the magnetic saturation of the sintered alloy, but also substantially increased its electrical resistivity. The magnetic saturation of the sintered alloy was superior to most powder-sintered iron-base soft magnetic materials. Additionally, the high electrical resistivity could also reduce the total power loss of the magnetic material at high-frequency alternative magnetic field by reducing the eddy-current loss. Controlling the phosphorous concentration by modifying the electroless plating parameters has the potential to improve the properties of sintered soft magnetic materials.

References

1. P. Lindskog, J. Tengzelius, and S.A. Kvist, Phosphorous as an Alloying Element in Ferrous P/M, *Modern Developments in Powder Metallurgy,* Vol 10, H.H. Hausner and P.V. Taubenblat, Ed., Metal Powder Industries Federation, 1977, p 97-128
2. M. Gagne, J.P. Poirier, and Y. Trudel, Designing a Steel Powder for Soft Magnetic Applications, *Advances in Powder Metallurgy,* Vol 2, E.R. Andreotti and P.J. McGeehan, Ed., Metal Powder Industries Federation, 1990, p 407-420
3. J. Kaczmar and B. Weglinski, Influence of Processing Parameters on Magnetic Properties of Fe-0.8P Sintered Materials, *Powder Metall.,* Vol 27, 1984, p 9-13
4. B. Weglinski and J. Kaczmar, Effect of Fe_3P Addition on Magnetic Properties of Sintered Iron, *Powder Metall.,* Vol 23, 1980, p 210-216
5. C. Lall, The Effect of Sintering Temperature and Atmosphere on the Soft Magnetic Properties of P/M Materials, *Advances in Powder Metallurgy & Particulate Materials,* Vol 3, J.M. Capus and R.M. German, Ed., Metal Powder Industries Federation, 1992, p 129-156
6. C. Lall and L.W. Baum, High Performance Soft Magnetic Components by Powder Metallurgy and Metal Injection Molding, *Modern Developments in Powder Metallurgy,* Vol 18, P.U. Gummeson and D.A. Gustafson, Ed., Metal Powder Industries Federation, 1988, p 363-389
7. C. Lall, *Soft Magnetism: Fundamentals for Powder Metallurgy and Metal Injection Molding,* Metal Powder Industries Federation, 1992, p 67-70
8. T.-Y. Chan and S.-T. Lin, Sintering of Elemental Carbonyl Iron and Carbonyl Nickel Powder Mixtures, *J. Mater. Sci.,* Vol 32, 1997, p 1963-1967
9. X. Qu, S. Gowri, and J.A. Lund, Sintering Behavior and Strength of Fe-Si-P Compacts, *Int. J. Powder Metall.,* Vol 27, 1991, p 9-13
10. R.M. German, *Liquid Phase Sintering,* Plenum Press, 1985, p 84-85, 184-185
11. Y.H. Chiou and S.T. Lin, Influences of Powder Preparation Routes on the Sintering Behaviour of Doped ZrO_2-3 mol%Y_2O_3, *Ceram. Int.,* Vol 23, 1997, p 171-177
12. B.V. Nitta, M.H. Morgan, and L. Kinna, Liquid Phase and Vapor Phase Deposition Techniques for Coating Metals on Metallic/Non-Metallic Powders, *Advances in Powder Metallurgy & Particulate Materials,* Vol 7, J.M. Capus and R.M. German, Ed., Metal Powder Industries Federation, 1992, p 89-99
13. C.A. Loto, Electroless Nickel Plating of Iron Powders, *J. Met.,* Vol 39, 1987, p 36-38
14. W. Riedel, *Electroless Nickel Plating,* ASM International, 1991, p 5-8, 40-44
15. C.J. Smithells and E.A. Brandes, *Metal Reference Book,* 5th ed., Butterworths, 1977, p 609, 730
16. H. Baker, *Alloy Phase Diagrams,* Vol 3, *ASM Handbook,* ASM International, 1992, p 2.200, 2.313
17. R.S. Tebble and D.J. Craik, *Magnetic Materials,* Wiley-Interscience, 1969, p 102-103
18. D.R. Lide, *CRC Handbook of Chemistry and Physics,* 73rd ed., CRC Press, 1992, p 4-66